Silikáty *31*, s. 193—205 (1987)

Původní práce

TEMPERATURE FIELDS CLOSE TO THE ELECTRODE SURFACE IN GLASS MELT

MILOSLAV NĚMEČEK

Electrotechnical Faculty of the Czech Technical University (ČVUT)
166 27 Prague 6, Suchbátarova 2

Received 15. 12. 1986

Knowledge of the temperature fields in the immediate proximity of the surface of electrodes is a necessary prerequisite of investigations concerned with corrosion and other processes taking place at the electrodes in glass melts.

Comprehensive data for this purpose can be obtained by means of simple mathematical models which contain equations (3) and (5); the latter also involves convective flow described by the uniform velocity profile. The analytical solution (7) of equation (3) describes the temperature field (Fig. 1) in motionless glass melt. Equations (3) and (5) were resolved numerically with the use of the finite differences method and the uniform profile of dimensionless velocity $f(\eta)$ was applied. The effect of the ky product is shown in Figs. 1 and 2 (equation (3)), the role of velocity and that of the exponents in equations (11a, b) and (12a, b) is illustrated by Figs. 3 through 10. The influence of harmonic 50 Hz current supply can be seen in Fig. 11 showing the time development of the temperature field.

INTRODUCTION

The temperature field in a glass melt affects a number of parameters in the melting process, especially those of thermal convective flow and of the intensity of chemical and physical reactions on the electrode surface or in the zones supplied with heated and overheated glass melt, i.e. those in the lower parts of the batch blanket and at the tank walls. From the point of view of technology, these parameters are associated with the tank output and the quality of the glass being melted, and can influence the corrosion of electrodes and of the refractory materials close by. However, additional phenomena due to non-isothermal conditions in the glass melt cannot be ruled out.

It is difficult to establish experimentally authentic values of temperature close to the electrode surface [1, 2]. The methods based on mathematical models seem to be more convenient in this respect [3, 4, 5]. For this purpose it is necessary to use a refined mesh module at small distances from the electrode surface. Unfortunately, this measure increases the computing costs. On the other hand, the probable occurence of fluctuations of temperature and velocity in the thermal convective flow makes the results of experimental investigations of the fields of temperature, velocity and electric potential more reliable.

However, if the fluctuations caused by natural convection can be regarded as being slow and of low intensity, the heat transfer process close to the electrode surface can be described by the steady state energy equation, and qualitatively valid results of its solutions can be expected.

The temperature fields adjacent to the electrode surface were resolved mathematically in order to obtain informative data for future research of the electrode

corrosion phenomena. A simple model in the simple cylindrical coordinate system was chosen and resolved both analytically and numerically.

The finite differences method was used in the numerical solutions. As no reliable data on the velocity field of thermal convection at vertical cylinders were available, the 'piston' shape of the dimensionless velocity profiles $f(\eta)$ [6] was introduced.

Estimation of the influence of thermal convective flow on the shape of the temperature field close to the electrode surface will in future allow the quantitative shares of the respective driving forces of thermal convection caused by the electrodes, the cold batch blanket and the tank inner walls to be assessed.

Further utilization of the computing outputs may even be aimed at investigating the electrodynamic forces involved in the surface movement of the glass melt at the electrode surface and contributing to the corrosion of electrodes. The certain inconvenient properties of the cylindrical shape of the energy equation, associated with the choice of boundary conditions, have to be tolerated for the sake of simplicity of the problem formulation.

THEORETICAL

The temperature field close to the electrode surface can be approximately described by the steady state energy equation written in cylindrical coordinates,

$$\varrho c \left(v_r \frac{\partial T}{\partial r} + v_z \frac{\partial T}{\partial z} \right) = k \left(\frac{\partial^2 T}{\partial z^2} + \frac{\partial^2 T}{\partial r^2} + \frac{1}{r} \frac{\partial T}{\partial r} \right) + \gamma \mathbf{EE}. \tag{1}$$

Because the electric field close to the electrode surface shows rotational symmetry, and if the current i_1 Am^{-1} is distributed uniformly over the unit length (lm) of the electrode, the term $\gamma \mathbf{EE}$ of equation (1) can be expressed in the simplified form

$$i_1 = 2\pi r_{el} \mathbf{J}_{el} \doteq 2\pi r \mathbf{J} = 2\pi \gamma r \mathbf{E}. \tag{2}$$

Thus, the temperature field in a motionless liquid can be described by the equation

$$\frac{\mathrm{d}^2 T}{\mathrm{d}r^2} + \frac{1}{r} \frac{\mathrm{d}T}{\mathrm{d}r} + \left(\frac{i_1}{2\pi} \right)^2 \frac{1}{\gamma k r^2} = 0. \tag{3}$$

which is independent of the electric field shape farther apart from the electrode surface.

If the liquid flows parallel with the axis of a vertical electrode, the following equation can be written for the region close to the electrode surface:

$$v_r \frac{\partial T}{\partial r} + v_z \frac{\partial T}{\partial z} = k(\varrho c)^{-1} \left(\frac{\partial^2 T}{\partial r^2} + \frac{1}{r} \frac{\partial T}{\partial r} + \frac{\partial^2 T}{\partial z^2} \right) + (\gamma \varrho c)^{-1} \left(\frac{i_1}{2\pi} \right)^2 r^{-2} \tag{4}$$

Its simplified form can be written as follows:

$$v_z \frac{\partial T}{\partial z} = \frac{k}{\varrho c} \left[\left(\frac{\partial^2 T}{\partial r^2} + \frac{1}{r} \frac{\partial T}{\partial r} + \frac{\partial^2 T}{\partial z^2} \right) - \frac{\varrho c}{k} v_r \frac{\partial T}{\partial r} \right] + (\gamma \varrho c)^{-1} \left(\frac{i_1}{2\pi} \right)^2 r^{-2} = 0, \tag{5}$$

which holds under the conditions

$$\frac{\partial^2 T}{\partial z^2} \ll \frac{\partial^2 T}{\partial r^2} + \frac{1}{r} \frac{\partial T}{\partial r} \tag{5a}$$

and

$$v_z(r = r_{el}) \neq 0. \tag{5b}$$

If it is desirable to know the shape of the field of electric potential Φ, one has to resolve the equation

$$\nabla (\gamma(-\nabla\Phi)) = 0. \tag{6a}$$

If $\boldsymbol{E} = -\nabla\Phi$, it acquires the following form in cylindrical coordinates:

$$\frac{\partial\gamma}{\partial r}\frac{\partial\Phi}{\partial r} + \frac{\partial\gamma}{\partial z}\frac{\partial\Phi}{\partial z} + \gamma\left(\frac{\partial^2\Phi}{\partial r^2} + \frac{1}{r}\frac{\partial\Phi}{\partial r} + \frac{\partial^2\Phi}{\partial z^2}\right) = 0. \tag{6b}$$

and for our purposes it can be written that

$$\frac{\partial\gamma}{\partial r}\frac{\partial\Phi}{\partial r} + \gamma\left(\frac{\partial^2\Phi}{\partial r^2} + \frac{1}{r}\frac{\partial\Phi}{\partial r}\right) = 0. \tag{6}$$

The condition (2) of the conservation of electric current is, of course, valid.

Equations (3), (5) and (6) were conveniently used to solve the practical problems shown in the paragraphs below.

TEMPERATURE FIELD

If equation (6) of the steady state potential field with the temperature dependent parameters is to be resolved, the temperature field has to be known. The most available information is provided by analytical solution of equation (3) wherein the product γk is independent of temperature. The solution of equation (3) has then the form

$$T = C_1 + C_2 \ln r - I_0 \ln^2 r, \tag{7}$$

where

$$I_0 = \frac{1}{2}\left(\frac{i_1}{2\pi}\right)^2 \frac{1}{\gamma k} \tag{7a}$$

and the various shapes of the temperature field can be studied for the various boundary conditions.

The other more general problems of non-isothermal fields must be solved by numerical methods.

a) Let us first study the effect of the thermal conductivity coefficient k ($\mathrm{Wm^{-1}\,K^{-1}}$) on the cylindrical temperature field close to the electrode surface (eq. (7)). The solutions for Dirichlet's boundary conditions $T_{el} = 1573$ at $r = r_{el} = 0.025$ m, $T_R = 1573$ K, 1673 K, 1773 K at $r = R = 0.4$ m, are plotted as curves 1—11 in Fig. 1 for various k values. These and the other parameters are listed in Table I.

Table I

Curve No.	1	2	3	4	5	6	7	8	9	10	11
k	10 $\mathrm{Wm^{-1}\,K^{-1}}$							7.5	15	10	
γ	21.05 $\mathrm{Sm^{-1}}$										
$10^{-3}\,J_{el}$	12.8 $\mathrm{Am^{-2}}$				11.5	9.6	11.5	12.8			

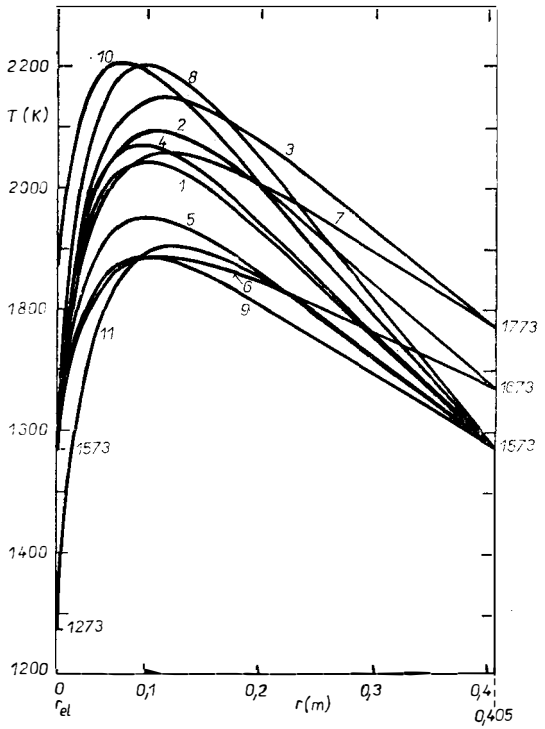

Fig. 1. Temperature curves computed analytically from (7) at various boundary conditions and conductivity coefficients k and γ (Table I).

where the current density on the electrode surface is expressed as

$$J_{el} = \frac{i_1}{2\pi r_{el}} . \tag{8}$$

Additional simpler information on the effect of thermal conductivity is provided by Fig. 2. Here the curves 3, 2, 1 corresponding to the three values $k = 20$, 10, 5 $Wm^{-1} K^{-1}$ respectively, are plotted. The current density was $J_{el} = 12\,800$ Am^{-2}, the electrical conductivity $\gamma = 21.05$ Sm^{-1}. In this case, the temperature field was calculated numerically using the finite differences method. The given parameters correspond to those usually employed in glass melting practice.

The shape of the temperature curves is characterized by a steep temperature gradient over very small radial distances from the electrode surface. The peaks of the temperature maxima are sharper and move closer to the electrode surface with increasing thermal conductivity.

The temperature is less affected by the secondary boundary condition, i.e. temperature T_R at radius $R = 0.405$, than by current density and thermal conductivity.

b) Additional findings, mostly qualitative in nature, were obtained by investigations into the way the liquid flow affects the formation of the temperature

field along a vertical electrode. Free thermal convective flow and a velocity field in the radial direction were considered and described by the equation (ref. [6])

$$v_z(z) = f(\eta)\sqrt{\beta\varrho g z(T_m - T_R)}. \tag{9}$$

Although equation (9) holds for planar plates only, it was accepted as sufficiently representative for choosing the function

$$f(\eta) = f\left(\frac{r - r_{el}}{z}\left(\frac{Gr_z}{4}\right)^{\frac{1}{4}}\right) = \text{const.}$$

where the Grashof number is

$$Gr_z = \frac{\beta_e g z^3 (T_m - T_R)}{\nu^2}, \tag{10}$$

z is the longitudinal coordinate measured from the electrode foot,
T_m is the temperature maximum.

The value of $f(\eta)$ was chosen from the interval $0.007 < f(\eta) < 0.028$ corresponding to Prandtl numbers of $3000 < Pr < 500$ respectively for glass melt at about 1600 K. Equation (5) was then resolved by the numerical finite differences method and the course of temperature profiles along coordinate z was computed. The course of the temperature profiles was based on the steady state conditions given in Fig. 2. In all the examples the current density at the electrode surface was

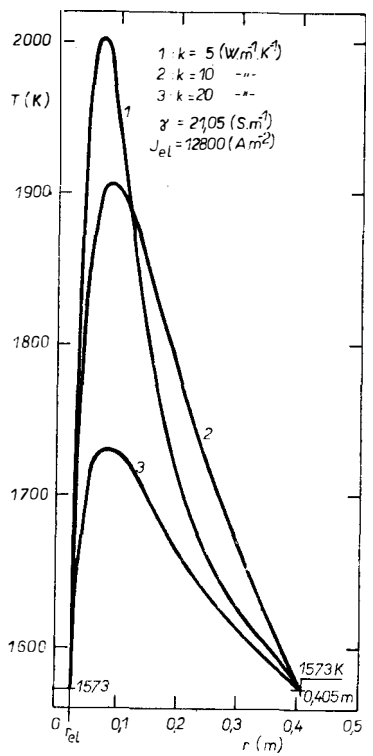

Fig. 2. Steady-state temperature curves in motionless glass melts having various thermal conductivity coefficients k. Computed from (3) by the finite differences method.

12 800 Am^{-2} but the electric and thermal conductivities were considered to be either constant or temperature-dependent, and expressed by equations

$$\gamma = 1.292 \times 10^{-12}\, T^{4.12} \qquad (Sm^{-1}) \tag{11a}$$

$$\gamma = 1.826\,96 \times 10^{-14}\, T^{4.7} \tag{11b}$$

and

$$k = 4 \times 10^{-6}\, T^{2} \tag{12a}$$

$$k = 9.9 \times 10^{-4\,1} T^{-15} \qquad (Wm^{-1}\,K^{-1}), \tag{12b}$$

for clear bottle and sheet glass respectively.

The dynamic viscosity of both types of glass was taken as

$$\mu = \varrho\nu = 2.9 \times 10^{44}\, T^{-13.45} \qquad (Pas). \tag{13}$$

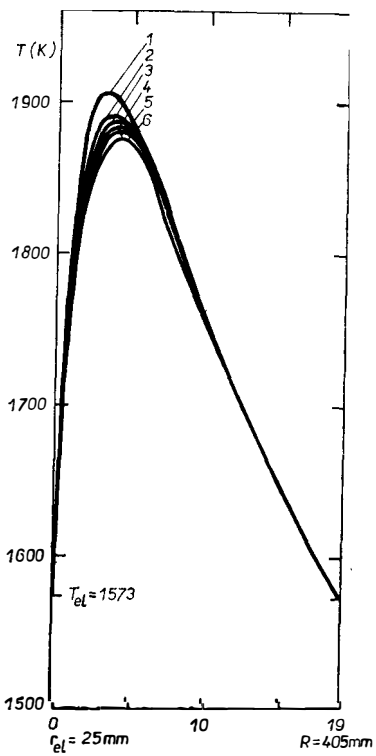

Fig. 3. Temperature curves at various vertical distances z from the foot of a vertical electrode having the diameter $2r_{el} = 50$ mm. Thermal convection is characterized by $f(\eta) = 0{,}01 = const.$ Thermal conductivity coefficient $k = 10$ $(Wm^{-1}K^{-1}) = const.$, the temperature-dependent electric conductivity coefficient $\gamma = 1{,}292 \,.\, 10^{-12} \,.\, T^{4.12}$ (Sm^{-1}). The numbers 1—6 correspond to the vertical coordinates z (m) as follows: 1: $z = 0 \div 0{,}04$, 2: $z = 0{,}08$, 3: $z = 0{,}2$, 4: $z = 0{,}4$, 5: $z = 0{,}6$, 6: $z = 1{,}0$. The temperature expansion coefficient $\beta_Q = 6 \,.\, 10^{-5}$ $(K^{-1}) = const.$ for all the glass types investigated (Figs. 3—11).

The radiation heat transfer was not considered in the temperature dependence of thermal conductivity. The electrode diameter was 50 mm in all the calculations. The results of the computations are plotted in Figs. 3 through 10, and allow the following conclusions to be formulated:

α) The convective flow shifts the temperature maxima away from the electrode surface and the maximum becomes less distinct with increasing z coordinate. The difference between temperature maxima at the foot and the tip of the electrode decreases with increasing flow velocity (Figs. 3 and 4).

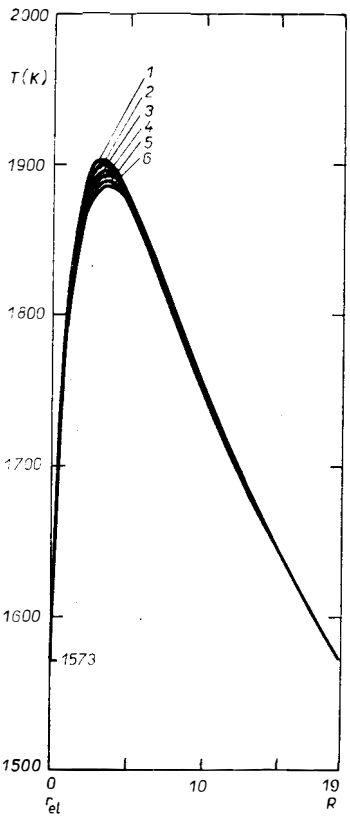

Fig. 4. Temperature curves 1—6 obtained if the thermal convection is more intensive, designed by $f(\eta)$ = = 0,022. All other parameters correspond to Fig. 3.

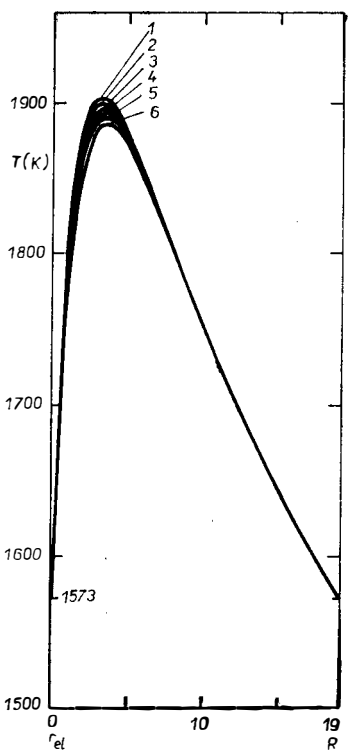

Fig. 5. Temperature curves 1—6 for the steeper temperature dependence of the electric conductivity coefficient $\gamma = 1{,}827 \cdot 10^{-14}\ T^{4.7}$ (Sm^{-1}). For the other parameters refer to Fig. 4.

β) The variability of the exponent over T in equations (12a, b) does not affect the shape of the developing temperature profiles (Figs. 4 and 5) insofar as the current density and the bulk melt temperature T_R do not change.

γ) In the case of low-intensity thermal convection, which was considered, the right-hand branches of the curves in Figs. 3, 4 and 5 are approximately identical.

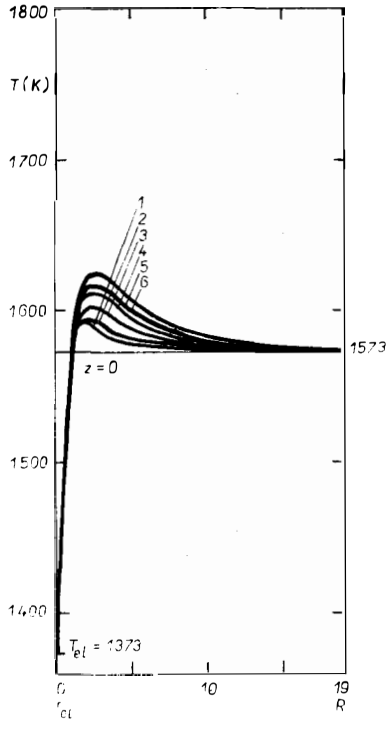

Fig. 6. Reversed sequence of temperature curves 1—6 obtained by changed boundary conditions. The radial transport of hot glass melt to the cold electrode surface was simulated by a high melt bulk temperature T_R. Parameters: $f(\eta) = 0{,}01$, $k = 10{,}24$ $(Wm^{-1}K^{-1})$, $\gamma = 21{,}05$ (Sm^{-1}), $\beta_\varrho = 6 \cdot 10^{-5}$ (K^{-1}).

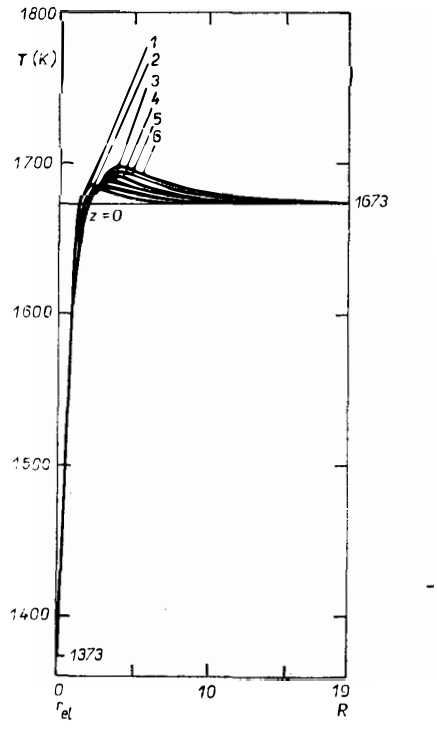

Fig. 7. Temperature curves 1—6 influenced by increase in bulk temperature to 1 673 K without changing the parameters of Fig. 6.

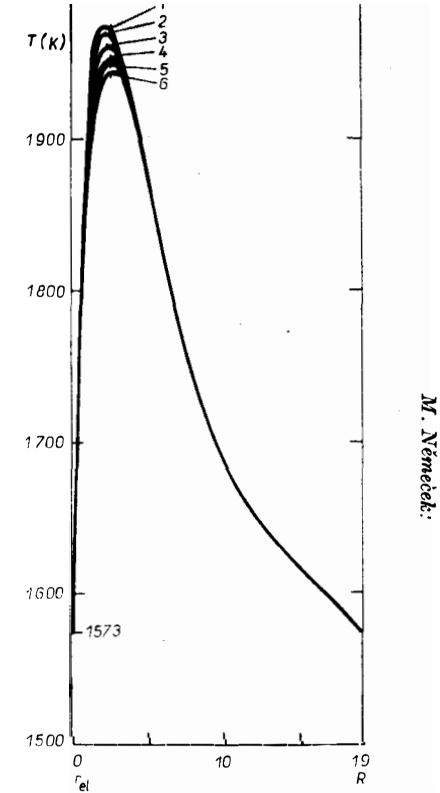

Fig. 8. Temperature curves 1—6 at $f(\eta) = 0{,}01$, $\gamma = 21{,}05$ (Sm^{-1}), $\beta_\varrho = 6 \cdot 10^{-5}$ (K^{-1}), obtained for temperature-dependent thermal conductivity coefficient $k = 9{,}9 \times 10^{-4} \cdot T^{1{,}15}$ $(Wm^{-1}K^{-1})$.

δ) The influence of thermal conductivity of the melt on the shape of the temperature profiles is illustrated by Figs. 8 and 9. Lower thermal conductivity shifts the temperature maxima closer to the electrode surface and causes the temperature difference along the electrode axis to increase. The effect of the exponents in equations (12a, b) follows from a comparison of Figs. 8 and 9.

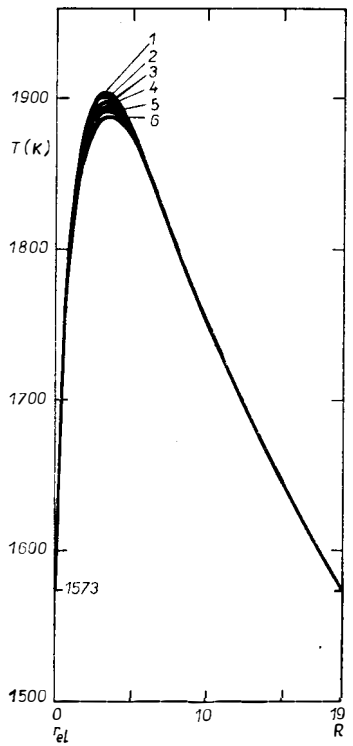

Fig. 9. Temperature curves 1—6 decreasing in case of steeper temperature dependence of thermal conductivity coefficient $k = 4 \cdot 10^{-6} \cdot T^2$ $(Wm^{-1}K^{-1})$ *without changing the other parameters from Fig. 8.*

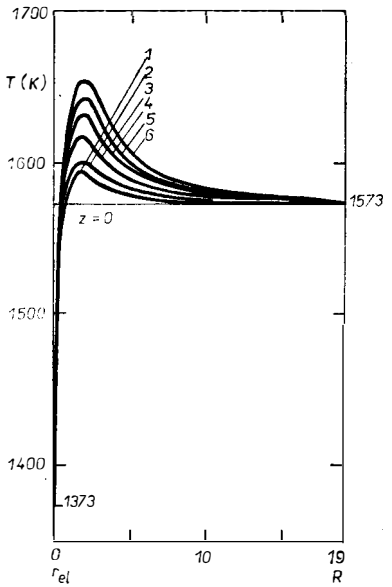

Fig. 10. Temperature curves 1—6 pertaining to a low thermal conductivity coefficient $k = 9{,}9 \cdot 10^{-4} \cdot T^{1{,}15}$ $(Wm^{-1}K^{-1})$. *The other parameters are:* $f(\eta) = 0{,}01$, $\gamma = 21{,}05$ (Sm^{-1}), $\beta_\varrho = 6 \cdot 10^{-5}$ (K^{-1}).

ε) The case of the surrounding liquid flowing intensively in the radial direction towards the foot of the electrode was simulated by the uniform boundary condition $T = \text{const.} = 1573$ K or 1673 K at $z = 0$ (Figs. 6, 7 and 10). The shape of the curves implies an immense heat flux towards the electrode surface in the case of rising temperature of the surrounding liquid. However, in this instance the temperature differences along the electrode axis were not taken into account. The decreased value of the thermal conductivity coefficient k (Fig. 10), corresponding to an opaque liquid, i.e. coloured glass, causes both the temperature gradient at the electrode surface and the respective heat flux to increase. The change in the melt thermal conductivity does not affect the remote parts of the temperature field.

ζ) All the examples given above apply to AC supply where the alternating current is represented by its effective value

$$i = \frac{i_1}{2\pi}\left(\int_0^{2\pi} \sin^2 \omega t \, \mathrm{d}t\right)^{\frac{1}{2}},$$

where $\omega = 2\pi f$; f (s^{-1}) is the frequency, i.e. 50 Hz.

The temperature fluctuations caused by harmonic oscillations of the 50 Hz electric current were also studied. The onset of the heating process close to the electrode surface is plotted in Fig. 11. The temperature oscillations at various distances from the electrode surface are apparent, as in the progressive attenuation of the oscillations in terms of the increasing radial coordinate.

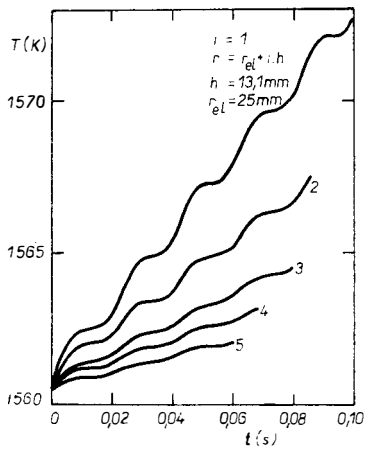

Fig. 11. Temperature oscillations caused by alternating electrical current supply of the electrode at distance i . h from its surface. The onset of the heating process in motionless glass melt $f(\eta) = 0$ at $J_{el} = 12\,800$ (Am^{-2}), $k = 10$ ($Wm^{-1}K^{-1}$) = const., $\gamma = 21{,}05$ (Sm^{-1}) = const.).

FUTURE

In spite of the great progress achieved so far in the description of temperature fields in glass melts, it cannot be said that all the problems have been resolved. A number of questions connected with the corrosion of electrode materials and with some general electrochemical problems have yet to be answered.

The problem of flow fluctuations under the conditions of thermal convection, and of their interpretation in mathematical models, particularly under suitable boundary conditions, also remains open. The extent of the effect of flow fluctuation on the corrosion processes is likewise not yet known.

At present, however, it can be assumed that the principal range of knowledge has already been gained. After its precisioning it should be possible to design more efficiently large glass tank furnaces which would be much less damaging to the environment.

References

[1] Zhi-Hao Zhon et al.: *Conference on Electric Melting of Glass*, Prague 1986, pp. 161—179.
[2] Ganzala G. W., Maddux J. F.: IEEE, Trans. Ind. Appl., ISA — 78, (1980), p. 966.
[3] Curran R. L.: IEEE, Trans. Ind. Appl., Vol. IA — 9, No 3, May/June 1973.
[4] Curran R. L.: IEEE Trans. Ind. Appl., IGA — 7, 1 (1971), pp. 116—129.
[5] Němeček M., Štefan J., Skřivan M.: Silikáty *24*, 59 (1980).
[6] Gebhart B.: *Heat Transfer*, McGraw-Hill Book Company, New York 1961.

List of Symbols

c specific heat (J kg^{-1} K^{-1})
C constant
f frequency (s^{-1}), function f' in [6]
Gr Grashof number
h length (m, mm)
i_l electric current (A/m) at 1 m length of the electrode bar
J_{el} electric current density (Am^{-2})
E intensity of electric field (Vm^{-1})
g gravity (m s^{-2})
k thermal conductivity coefficient (Wm^{-1} K^{-1})
r radial coordinate (m)
r_{el} electrode radius (m)
R boundary radius (m)
t time (s)
T temperature (K)
v velocity (m s^{-1})
z longitudinal coordinate (m)
β_e temperature expansion coefficient of glass (K^{-1})
γ electric conductivity coefficient (Sm^{-1})
η dimensionless coordinate [6]
μ dynamic viscosity (kg m^{-1} s, Pas)
ν kinematic viscosity (m^2 s^{-1})
ϱ density (kg m^{-3})
Φ electric scalar potential (V)
ω circular frequency (s^{-1})

Indices

el electrode surface
m maximum
r radial
R at $r = R$
z longitudinal

TEPLOTNÍ POLE VE SKLOVINĚ U POVRCHU ELEKTROD

Miloslav Němeček

ČVUT, Fakulta elektrotechnická, 166 27 Praha 6

Teplotní pole blízko k povrchu elektrody bylo popsáno rovnicemi (3) a (5) v cylindrických souřadnicích. Analytické řešení (7) rovnice (3) poskytlo informaci o teplotním poli (obr. 1 a tabulka I) v nepohyblivé sklovině kolem vertikální elektrody s dodávaným proudem i_1 (Am^{-1}). Rovnice (3) a rov. (5) byly řešeny numericky užitím metody konečných diferencí. V případě pohybující se skloviny byl v rov. (5) předpokládán „pístový" profil bezrozměrné rychlosti $f(\eta)$. Vliv součinu $\gamma . k$ elektrické a tepelné vodivosti je zřejmý z obr. 1 a 2 (pro rov. (3)), vliv strmosti elektrické a tepelné vodivosti (vztahy (11a, b) a (12a, b)) a vliv rychlosti volné konvekce podél vertikální elektrody je patrný z obr. 3 až 10. Vliv harmonického kolísání elektrického proudu 50 Hz tekoucího do elektrody, v různých vzdálenostech od jejího povrchu, je patrný z obr. 11, kde je znázorněn časový vývoj procesu.

Obr. 1. Teplotní křivky vypočtené analyticky (rov. 7) za různých okrajových podmínek a vodivostí k a γ (tab. I).

Obr. 2. Stacionární teplotní křivky v nepohyblivé sklovině při třech různých tepelných vodivostech k. Vypočteno z (3) metodou konečných diferencí.

Obr. 3. Teplotní křivky v různých výškách z od paty vertikální elektrody o průmcru $2r_{el} = 50$ mm. Teplotní konvekce je vyjádřena činitelem $f(\eta) = 0{,}01 = konst.$ Tepelná vodivost $k = 10$ ($Wm^{-1}K^{-1}$) = konst., elektrická vodivost (konduktivita) = $1{,}292 . 10^{-12} T^{4{,}12}$ ($S m^{-1}$) je teplotně závislá. Číslice 1 až 6 odpovídají výškám z (m) takto: 1: z = 0—0,04; 2: z = 0,08; 3: z = 0,2; 4: z = 0,4; 5: z = 0,6; 6: z = 1. Součinitel teplotní objemové rozpínavosti $\beta_\varrho = 6 . 10^{-5}$ (K^{-1}) = konst. pro všechny zkoumané skloviny v obr. 3 až 11.

Obr. 4. Teplotní křivky 1 až 6 získané při intenzivnější teplotní konvekci vyjádřené $f(\eta) = 0{,}022$. Ostatní parametry odpovídají obr. 3.

Obr. 5. Teplotní křivky 1 až 6 pro strmější teplotní závislost elektrické vodivosti (konduktivity) $\gamma = 1{,}827 . 10^{-14} . T^{4{,}7}$ (Sm^{-1}). Ostatní parametry viz obr. 4.

Obr. 6. Obrácený sled teplotních křivek 1 až 6 získaný změnou okrajových podmínek. Radiální přísun horké skloviny k chladnému povrchu elektrody je simulován vyšší teplotou okolí. Parametry: $f(\eta) = 0{,}01$; $k = 10{,}24$ ($Wm^{-1}K^{-1}$); $\gamma = 21{,}05$ (Sm^{-1}), $\beta_\varrho = 6 . 10^{-5}$ (K^{-1}).

Obr. 7. Teplotní křivky 1 až 6 ovlivněné zvýšením okolní teploty na 1 673 K, parametry z obr. 6 nezměněny.

Obr. 8. Teplotní křivky 1 až 6 pro $f(\eta) = 0{,}01$; $\gamma = 21{,}05$ (Sm^{-1}); $\beta_\varrho = 6 . 10^{-5}$ (K^{-1}) získané při teplotně závislé tepelné vodivosti $k = 9{,}9 . 10^{-4} T^{1{,}15}$ ($Wm^{-1}K^{-1}$),

Obr. 9. Teplotní křivky 1 až 6 pro strmější teplotní závislost $k = 4 . 10^{-6} T^2$ ($Wm^{-1}K^{-1}$). Ostatní parametry obr. 8 nezměněny.

Obr. 10. Teplotní křivky 1 až 6 vztažené k nízké tepelné vodivosti $k = 9{,}9 . 10^{-4} T^{1{,}15}$ ($Wm^{-1}K^{-1}$) při $f(\eta) = 0{,}01$; $\gamma = 21{,}05$ (Sm^{-1}); $\beta_\varrho = 6 . 10$ (K^{-1}).

Obr. 11. Teplotní kmity vyvolané napájením elektrody střídavým proudem 50 Hz ve vzdáleoosti i . h od jejího povrchu. Je zobrazen rozběh procesu v klidné sklovině —$f(\eta) = 0$ při $J_{el} = 12\,800$ (Am^{-2}); $k = 10$ ($Wm^{-1}K^{-1}$) = konst.; $\gamma = 21{,}05$ (Sm^{-1}) = konst.

ТЕМПЕРАТУРНОЕ ПОЛЕ В СТЕКЛОМАССЕ У ПОВЕРХНОСТИ ЭЛЕКТРОДОВ

Милослав Немечек

ЧВУТ, Электротехнический факультет, 166 27 Прага 6

Температурное поле в непосредственной близости к поверхности электрода было описано уравнениями (3) и (5) в цилиндрических координатах. Аналитическое решение (7) ур. (3) дает образ о температурном поле (рис. 1 и табл. 1) в неподвижной стекломассе вблизи вертикального электрода нагруженного электрическим током. Уравнения (3) и (5)

решены нумерически с использованием метода конечных дифференций. Если стекломасса движущая, для ее предполагается в ур. (5) плоский профиль безразмерной скорости $f(\eta)$. Влияние продукта $\gamma \cdot \kappa$ электрической и тепловой проводностей показывают рис. 1 и 2 (для ур. (3)), влияние формы кривых электро- и теплопроводности (11а, б) и (12а, б), совместно с влиянием скорости свободной конвекции показано в рисунках 3—11. Влияние гармонического колебания эл. тока 50 Hz подводимого в электрод на колебания температуры в разных отстояниях от поверхности электрода показан на рис. 11 в начале развития процесса.

Фиг. 1. Кривые температуры из аналитического решения (7) *для разных краевых условий и коэффициентов* k *и* γ (*табл. 1*) *тепловой и электрической проводностей.*

Фиг. 2. Стационарные кривые температуры в неподвижной стекломассе для трех разных теплопроводностей k. *Исчислено из* (*3*) *по методу конечных дифференций.*

Фиг. 3. Кривые температуры в разных высотах z *от базы вертикального электрода диаметром* $2r_{el} = 50$ (mm). *Тепловая конвекция характеризуется фактором* $f(\eta) = 0{,}01 = конст$. *Коэффициент теплопроводности* $k = 10$ (W . m^{-1} . K^{-1}) = *конст., к. эл. проводности* $\gamma = 1{,}292 \cdot 10^{-12} \cdot T^{4.12}$ (S . m^{-1}) *зависит от температуры. Обозначения 1—6 присутствуют высотам* $z(m)$: *1:* $z = 0$—$0{,}04$; *2:* $z = 0{,}08$; *3:* $z = 0{,}2$; *4:* $z = 0{,}4$; *5:* $z = 0{,}6$; *6:* $z = 1$. *Коэффициент объемного растяжения* $\beta_\varrho = 6 \cdot 10^{-5}$ (K^{-1}) = *конст для всех исследованых сортов стекломассы в фиг. от 3 до 11.*

Фиг. 4. Кривые температуры 1—6 для более крутой температурной зависимости электрической проводности $\gamma = 1{,}827 \cdot 10^{-14} \cdot T^{4{,}7}$ (S . m^{-1}), *с остальными параметрами соответственно фиг. 4.*

Фиг. 5. Кривые температуры 1—6 для более крутой температурной зависимости электрической проводности $\gamma = 1{,}827 \cdot 10^{-14} \cdot T^{4{,}7}$ (S . m^{-1}) *с остальными параметрами соответственно фиг. 4.*

Фиг. 6. Обратная последовательность кривых 1—6 под влиянием изменения краевых условий. Подвод горячей стекломассы в радиальном направлении к холодной поверхности электрода симулируется более высокой температурой стекломассы около электрода. Параметры: $f(\eta) = 0{,}01$; $k = 10{,}24$ (W . m^{-1} . K^{-1}); $\gamma = 21{,}05$ (S . m^{-1}); $\beta_\varrho = 6 \cdot 10^{-5}$ (K^{-1}).

Фиг. 7. Кривые температуры 1—6 под влиянием повышения температуры стекломассы до 1 673 K, параметры из фиг. 6 остават.

Фиг. 8. Кривые температуры 1—6 для $f(\eta) = 0{,}01$; $\gamma = 21{,}05$ (S . m^{-1}); $\beta_\varrho = 6 \cdot 10^{-5}$ (K^{-1}) *для зависимого от температуры коэффициента теплопроводности* $k = 9{,}9 \cdot 10^{-4} \cdot T^{1.15}$ (W . m^{-1} . K^{-1}).

Фиг. 9. Кривые температуры 1—6 для более крутой температурной зависимости коэффициента теплопроводности $k = 4 \cdot 10^{-6} \cdot T^2$ (W . m^{-1} . K^{-1}). *Остальные параметры соответственно фиг. 8.*

Фиг. 10. Кривые температуры для низкого значения коэффициента теплопроводности $k = 9{,}9 \cdot 10^{-4} \cdot T^{1{,}15}$ (W . m^{-1} . K^{-1}) *при* $f(\eta) = 0{,}01$; $\gamma = 21{,}05$ (S . m^{-1}); $\beta_\varrho = 6 \cdot 10^{-5}$ (K^{-1}).

Фиг. 11. Колебания температуры под влиянием переменного эл. тока 50 Hz в радиальных отстояниях $i \cdot h$ *от поверхности электрода. Изображены начальные периоды процесса в неподвижной стекломассе —* $f(\eta) = 0$, *при* $J_{el} = 12\,800$ (A . m^{-2}), $k = 10$ (W . m^{-1} . K^{-1}) = *конст*, $\gamma = 21{,}05$ (S . m^{-1}) = *конст.*

Zajímavosti

VÝZKUMNÉ PROGRAMY V OBORU SKLA NA UNIVERZITÁCH USA. Redakce časopisu Ceramic Bulletin požádala univerzity USA o zveřejnění jejich současných výzkumných programů v oblasti silikátových, resp. materiálových věd a z odpovídajících inženýrských disciplín. (Ceramic Bulletin *64*, 1082 (1985).)

Ze 36 dotazovaných univerzit jich do uzávěrky odpovědělo 25 a zveřejnilo 446 hlavních výzkumných programů. Z tohoto počtu je asi 160 programů, které se týkají sklářství a příbuzných problematik, resp. některých obecnějších disciplín, majících aplikaci pro sklářství.